Diffusion and Interaction in Gels and Solutions. 3. Theoretical Results on the Obstruction Effect

Lennart Johansson* and Christer Elvingson

Department of Physical Chemistry, Chalmers University of Technology, S-412 96 Göteborg, Sweden

Jan-Erik Löfroth

Department of Drug Delivery Research, Pharmaceutical R&D, Astra Hässle AB, S-431 83 Mölndal, Sweden

Received March 4, 1991; Revised Manuscript Received May 24, 1991

ABSTRACT: A new theory for the diffusion of a spherical solute in a network, e.g., a polymer gel or solution, is presented. The distribution of spaces in the network is used to evaluate a frequency function giving the weights of cylindrical cells with different radii. Once the frequency function is known, the effective diffusion coefficient can be calculated, numerically or analytically, from the local diffusion coefficients given by the solution of Fick's first law in the cylindrical cell model. The predictions are compared with Brownian dynamics simulations, literature data, and results from our own experiments. It is found that the theory can successfully predict the diffusion of solutes in both flexible and stiff polymer systems. One result is that the diffusion of a solute is faster in a system of flexible polymers than in a system of stiff polymers. A crucial parameter is the ratio p/a, where p is the persistence length of the polymer and a is its radius. It is shown that the space distribution given by Ogston can be used to give a qualitative description of the hindrance when $p/a > 10$. However, in this case a quantitative prediction can also be made by the analytical theory presented here. When $p/a < 10$, a numerical calculation of the solute diffusion can be carried out. Thus, the approach in this paper leads to a theory with a wide range of applications.

Introduction

In Part 2 we described measurements of the translational diffusion of monodisperse poly(ethylene glycol) fractions (M_w in the range 300–4000), here denoted solute, in different polymer gels and solutions.[1] The results indicated that the hindrance due to the polymer chains depended not only on the size of the solute and the amount of polymer but also on the properties of the polymer chains, e.g., their thickness and stiffness. We also emphasized the need for a quantitative or at least semiquantitative explanation of our results.

Different approaches to describe diffusion data can been found in the literature. Several of these deal with hydrodynamics[2-4] and in the case of polymer systems these theories are often based on scaling concepts. Other theories are based on solutions of Fick's first law for different geometries,[5-8] while phenomenological approaches, e.g., the Ogston theory,[9] have also been used. However, none of these theories was able to give a consistent explanation of our experimental results.

Nevertheless, the underlying concept[10] of the Ogston theory, i.e., "spaces in a uniform random suspension of fibers", seems quite intuitive and has further been found to be valid by statistical mechanical means, both theoretically[11] and by Monte Carlo simulations.[12] Thus, it is tempting to apply the same idea to arbitrary arrangements of polymer chains and to obtain an appropriate expression for the diffusion quotient, D/D_0, given the structure of a polymer gel or solution. Here, D/D_0 is the quotient between the diffusion coefficients in a network and in a pure solvent, respectively.

A global D/D_0 can be described as the result of local flows in microscopic subsystems.[5] Further, the local diffusion coefficients can be obtained from the solution of Fick's first law in, e.g., the cylindrical cell model.[6,7] It is then necessary to find a frequency function, i.e., the weights, for the cylindrical cells, each with a certain cell radius. Here we will show a way to accomplish this and how the predictions compare with Brownian dynamics simulations and experiments.

* To whom correspondence should be addressed.

Theory

The so-called distribution of spaces in a random suspension of fibers can be calculated according to Ogston.[10] By this procedure, which is described in detail below, one obtains the probability distribution, $g(R)$, of spaces of size R. Thus, $g(R)$ is the probability that a randomly chosen point in a network of fibers is found at the radial distance R to the fiber of closest approach. Applying this technique to the cylindrical cell model (CC), which consists of an infinite cylindrical cell, containing solvent and polymer, with the polymer represented as a rod centered in the cell, one obtains $g(R)$ for one cylindrical cell as

$$g^{CC}(R) = \frac{2(R+a)}{b^2} S(R-(b-a)) \qquad (1)$$

Here a is the polymer radius and b is the cell radius, which is a function of the (local) polymer concentration. Furthermore, $S(R-(b-a))$ is a step function, which equals 1 if $R \leq b-a$ and 0 if $R > b-a$.

Let us now assume that we can describe $g(R)$ for any arbitrary network in terms of cylindrical cells and frequency functions $f(b)$, i.e., the weights of the different cells. Then we can write

$$g(R) = \int_a^\infty f(b)\, g^{CC}(R)\, db \sim \sum_b f(b)\, g^{CC}(R) \qquad (2)$$

The principle underlying eq 2 is illustrated in Figure 1 for a $g(R)$ calculated according to the Ogston theory. Accordingly, it should be possible to calculate $f(b)$ by deconvolution if $g(R)$ is known. This deconvolution is further discussed below; see Computational Methods.

0024-9297/91/2224-6024$02.50/0

Finally, the expectation value of the global D/D_0 is obtained as

$$\frac{D}{D_0} = \int_a^\infty f(b)\frac{D(b)}{D_0}\,db \tag{3}$$

where we use

$$\frac{D(b)}{D_0} = \frac{1}{1 + (R_s + a)^2/b^2} S(R_s-(b-a)) \tag{4}$$

for each cylinder. Equation 4 is the radial diffusion quotient (diffusion perpendicular to the polymer) for a neutral molecule in the cylindrical cell model,[6,7] modified to allow for a finite radius, R_s, of the diffusing species.

It must be stressed that the above procedure is applicable to any arbitrary $g(R)$, giving numerical results for $f(b)$ and D/D_0. On the other hand, if we have an analytical expression for $g(R)$, e.g., if we assume Ogstons's expression[10] to be valid, it is possible to obtain analytical solutions for $f(b)$ and D/D_0. We then start with Ogston's expression, modified to allow for a finite polymer radius

$$g(R) = \frac{2\phi(R + a)}{a^2} e^{-\phi(R+a)^2/a^2} \tag{5}$$

where ϕ is the volume fraction of the network. A solution to eq 2 with $g^{CC}(R)$ according to eq 1 is then given by

$$f(b) = \frac{2\phi^2 b^3}{a^4} e^{-\phi b^2/a^2} \tag{6}$$

D/D_0 can now be calculated according to eqs 3 and 4, with the use of the analytical result for $f(b)$, eq 6, resulting in

$$D/D_0 = e^{-\alpha} + \alpha^2 e^{\alpha} E_1(2\alpha) \tag{7}$$

where $\alpha = \phi(R_s + a)^2/a^2$ and E_1 is the exponential integral, i.e., $E_1(x) = \int_x^\infty e^{-u}/u\,du$.

In the following sections we will compare our predictions with Brownian dynamics simulations of sphere diffusion in computer-generated networks to test the accuracy of this approach. We will also show how the theory compares with literature data.

Computational Methods

Construction of Network. A discrete wormlike chain (wlc) model was used for the chains constituting the network. Each chain consisted of spherical subunits—beads—with a radius $a^* = 1.5^{1/2}a$, where a is the radius of the corresponding volume-adjusted cylinder. Chains with different flexibility were constructed by changing the persistence length, p, of the chain. The persistence length is related to the bending force constant k^b by[13]

$$k^b = \frac{pk_BT}{2a^*} \tag{8}$$

where T is the temperature and k_B is the Boltzmann constant. The distribution for the bond angles θ, assuming free rotation, is given by[14]

$$F(\theta_j) \sim \theta_j e^{-k^b\theta_j^2/2} \tag{9}$$

where θ_j is the bond angle between bonds j and $j-1$. The network was then obtained by first putting a bead at one of the sides of a cubic box. One bead at a time was then added at touching distance by sampling bond angles from the distribution defined by eq 9. When a subunit was added outside the box, a new side was chosen and the procedure was repeated until the desired volume fraction was reached. The last chain was always allowed to reach the side of the cube, modeling infinite chain lengths. For some cases the chains were not allowed to cross each other, and the overlapping chains were then discarded.

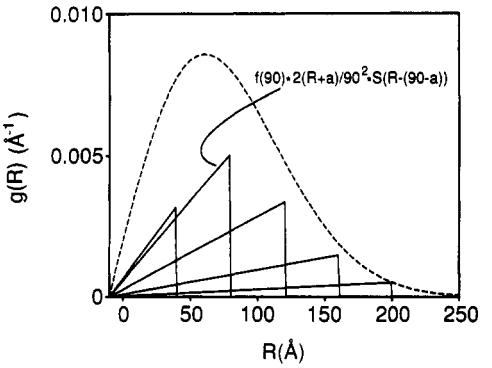

Figure 1. The underlying principle of eq 2. The dashed line is $g(R)$ according to eq 5, with $\phi = 0.01$ and $a = 10$ Å, and the solid lines are $f(b)$ $g^{CC}(R)$ for a set of cylindrical cells with $a = 10$ Å, each with a weight $f(b)$ and a cell radius b.

Distribution of Spaces in a Network. The probability distribution of spaces of size R, $g(R)$, was calculated as outlined in the preceding section. Points were chosen at random in the cubic box containing the network. The distance, R, to the bead of closest approach from each point residing outside a bead was sampled in a histogram generating $g(R)$. The interval spacing in the histogram was typically 1 Å. For each $g(R)$, 100 networks were generated and 3×10^4 random points were chosen in one such network. Finally, $g(R)$ was normalized by the total number of points and the interval spacing. The volume fraction of each network was calculated as the number of points located within the beads divided by the total number of points.

Closely related to the distribution of spaces is the partitioning of a solute between a solvent and, e.g., a gel phase or a polymer solution. We calculated the partition coefficient for small polymer chains, modeling the poly(ethylene glycol) (PEG) fractions used in experiments.[1] This was carried out by putting wlc chains into the network, using the same procedure as when generating the network. We then estimated the fraction of the modeled PEG chains that did not overlap with the network, using $\sim 10^4$ trials. This value was set equal to the partition coefficient. The small polymer chains consisted of 7–90 subunits, each with a radius equal to 3.1 Å, which was also used as the persistence length. The radius of gyration of the different PEG models in the networks was calculated according to

$$R_G = (\sum_i \langle s_i \rangle^2/n)^{1/2} \tag{10}$$

where s_i is the distance of the ith subunit from the center of mass of a polymer chain and n is the number of subunits.

Deconvolution Method. Knowing $g(R)$ numerically, a frequency function for cylindrical cells, $f(b)$, was evaluated by deconvolution, in accordance with eq 2. The numerical $g(R)$ had been sampled in q intervals with a spacing equal to ΔR. Thus, starting with the qth interval we had

$$f_q = g_q \frac{(q\Delta R + a)^2}{2((q - {}^1/_2)\Delta R + a)} \tag{11}$$

where g_q is associated with the midpoint value $R_q = (q - {}^1/_2)\Delta R$ of the qth interval and a is the known polymer radius. Using this starting value, f_q, it was then possible to obtain the entire frequency function by an iterative

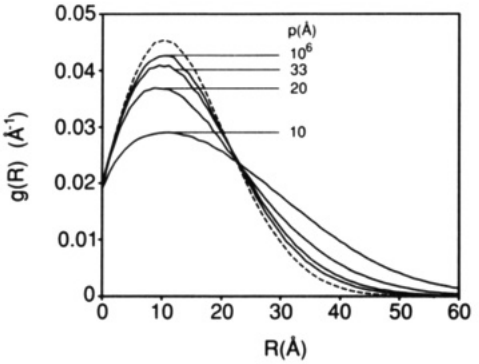

Figure 2. $g(R)$ for networks composed of nonoverlapping stiff chains ($p = 10^6$ Å) (dashed line) and of overlapping chains with different persistence lengths, p (solid lines). In all cases, we used $\phi = 0.026$ and $a = 3.3$ Å.

procedure, working through $i = q - 1$ to $i = 1$, using eq 12

$$f_i = g_i \frac{(i\Delta R + a)^2}{2((i - {}^1/_2)\Delta R + a)} - \sum_{j=i+1}^{q} \frac{(i\Delta R + a)^2}{(j\Delta R + a)^2} \qquad (12)$$

Here, f_i is the weight of the ith cylindrical cell, which has a cell radius $b_i = i\Delta R + a$. Finally, $f(b)$ was then normalized with ΔR, and D/D_0 was calculated numerically according to eqs 3 and 4.

Dynamic Simulations. The motion of a Brownian particle in a solvent can often be described by the Langevin equation[15]

$$\mathrm{d}\mathbf{p}(t)/\mathrm{d}t = -\zeta\mathbf{p}(t) + \mathbf{R}'(t) \qquad (13)$$

where $\mathbf{p}$ is the linear momentum, $\mathbf{R}'$ is a random force due to collisions with the solvent molecules, and ζ is a friction coefficient, which is related to the diffusion coefficient D_0 by $D_0 = kT/m\zeta$, m being the particle's mass. This, together with the fluctuation–dissipation theorem[15]

$$\zeta\langle p^2\rangle = \int_0^\infty \langle \mathbf{R}'(0)\cdot\mathbf{R}'(t)\rangle \, \mathrm{d}t \qquad (14)$$

then defines the average motion of a particle in a quiescent fluid. An algorithm for the motion of a particle during a time step Δt, for Δt large compared to the momentum relaxation time ζ^{-1}, was then obtained by sampling from a Gaussian distribution of random displacements

$$\Delta\mathbf{r}(t,\Delta t) = \mathbf{S}(\Delta t) \qquad (15)$$

where $\langle \mathbf{S}\rangle = 0$ and $\langle S_\alpha S_\beta\rangle = \delta_{\alpha\beta}(2D_0\Delta t)$. Greek indices denote Cartesian components, and δ is the Kroenecker delta. The effect of the network was taken into account by ignoring steps leading to overlap, i.e., treating the network beads as hard spheres. An infinite system was simulated by using periodic boundary conditions. From each trajectory a diffusion coefficient of the particle in the network, D, was obtained from a plot of $\langle \Delta r^2\rangle$ versus t and using the relation

$$\langle \Delta r^2\rangle = 6Dt \qquad (16)$$

A time step between 2.5 to 10.0 ps was used, and the reported diffusion quotients, D/D_0, were averages over 100 trajectories, each consisting of 1×10^6 to 8×10^6 accepted steps. All simulations were carried out in triplicate.

Results

We calculated the distribution of spaces in networks composed of chains with different flexibility, ranging from stiff chains, $p = 10^6$ Å, to random coils, $p = 10$ Å. It is seen in Figure 2 that as long as the ratio between the persistence length and the polymer radius, p/a, was larger than 10, the space distribution from each simulation was almost the same. On the other hand, decreasing the persistence length below this value created larger spaces. This is illustrated in Figures 3, and obviously the effect was due to polymer coiling. The difference between nonoverlapping and overlapping chains, modeling linear chains and cross-linked gels or branched chains, respectively, was quite small (see Figure 2). The result for the stiff overlapping chains was the same as that obtained with Ogston's expression, eq 5 (results not shown).

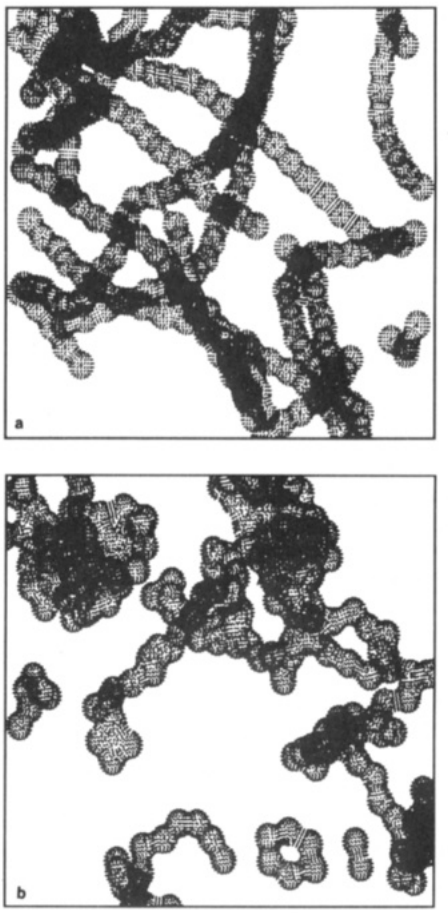

Figure 3. Selected chain configurations from our network simulations projected in two dimensions: (a) $p = 200$ Å, $\phi = 0.026$, and $a = 3.3$ Å; (b) $p = 10$ Å, $\phi = 0.026$, and $a = 3.3$ Å.

To get a quantitative estimation of these effects on the decrease of solute diffusion, we carried out Brownian dynamics (BD) simulations in two different networks. One was composed of stiff chains and the other of random coils. The results for the diffusion of spheres of different sizes are shown in Figure 4. The results showed that networks that had been built up by stiff chains created a greater hindrance to diffusion, i.e., the same effect as that expected from the simulated space distributions. Using our theory, here the numerical part, we were able to calculate D/D_0 for the two cases, and the predictions compared favorably with the BD simulations. Also, we have included the result of the phenomenological approach by Ogston et al.[9]

Our theoretical predictions were also compared with experiments. One of the most reliable sets of diffusion data in the literature has been obtained by Ogston et al.[9] They measured the diffusion of albumin in solutions of hyaluronic acid (HA) and dextran. From literature values, we calculated a polymer radius $a = 3.7$ Å for both the polymers, using $l\pi a^2 N_A/M_0 = v$, where v = partial specific

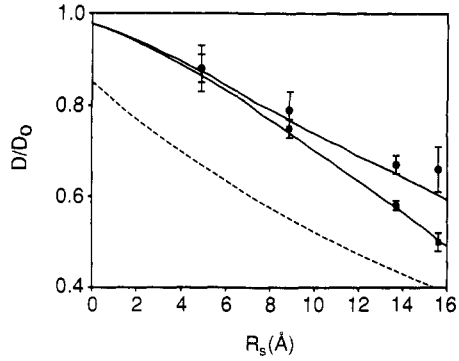

Figure 4. D/D_0 vs R_s from Brownian dynamics simulations in networks composed of stiff chains, $p = 10^6$ Å (squares), and flexible chains, p = 10 Å (circles). The solid lines are numerical predictions in accordance with eqs 2 and 3. The maximal standard deviation in these predictions (at R_s = 16 Å) amounted to 1.1% ($p = 10^6$ Å) and to 0.99% (p = 10 Å). The dashed line is the result from Ogston's phenomenological approach.[9] In all cases, we used ϕ = 0.026 and a = 3.3 Å.

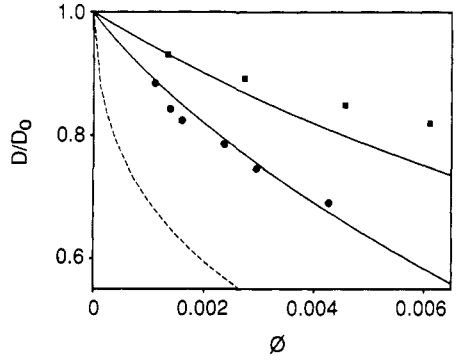

Figure 5. D/D_0 vs ϕ for experimental results[9] on the diffusion of albumin in solutions of hyaluronic acid (circles) and dextran (squares). The solid lines are predictions with our theory, and the dashed line is the result from Ogston's phenomenological approach.[9]

volume = 0.66 mL/g for HA[16] and 0.61 mL/g for dextran,[17] l = mean residue length = 10 Å for HA[18] and 3.89 Å for dextran,[17] and M_0 = residue weight = 401 for HA and 162 for dextran. According to the literature the persistence length of HA is larger than $10a$ = 37 Å.[16] Thus, we could apply our analytical theory, i.e., eq 7, for that case. For dextran, which is quite flexible, p is about 10 Å.[19] Consequently, we had to use numerical calculations. The results of these calculations are shown in Figure 5. Satisfactory agreement with the experiments was obtained, especially with the data for HA. The prediction with Ogston's approach[9] is also shown. In all the calculations, we used the value reported by Ogston for the radius of albumin, 35.5 Å, to which we added the diameter of one water molecule, 3.8 Å, obtaining R_s = 39.3 Å. This was an approximate way of accounting for the hydration of the HA and dextran chains, shown for example by eq 7, where $\alpha = \phi(R_s + a)^2/a^2$. Instead of recalculating ϕ when the water diameter was added to the polymer radius, it is seen that eq 7 can be rewritten as $\alpha = (R_s + a)^2/\langle b\rangle^2$ in terms of a cylindrical cell model with a mean cell radius equal to $\langle b\rangle$ ($=a/\phi^{1/2}$). Adding a constant value, e.g., 3.8 Å, either to a or to R_s is then equivalent.

Our experiments were carried out with poly(ethylene glycol) fractions.[1] As our theoretical arguments are based on the diffusion of spheres, we had to find an equivalent radius for the PEGs. Thus, we carried out computer simulations of the partitioning of a polymer, modeling PEG, between a solvent and a network composed of stiff

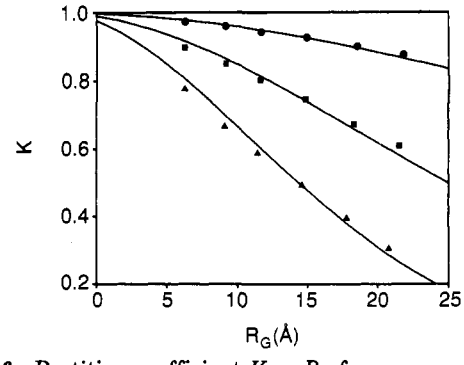

Figure 6. Partition coefficient K vs R_G from computer simulations of small polymers partitioning between a solvent and networks of different volume fractions ϕ = 0.0025 (circles), 0.010 (squares), and 0.026 (triangles). In all cases a = 3.3 Å and p = 10^6 Å. The lines are predictions of K for spheres with radius R_G.

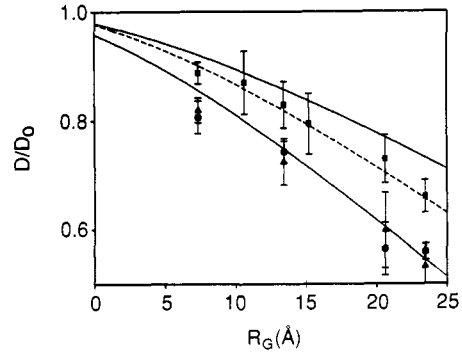

Figure 7. D/D_0 vs R_G for experimental results[1] on the diffusion of poly(ethylene glycol) in κ-carrageenan as a physically cross-linked gel (squares), as a solution (circles), and as a chemically cross-linked gel (triangles). The lines are predictions with our analytical theory, eq 7. The volume fraction ϕ was 0.01. See text for further details.

chains. In Figure 6, the simulated partition coefficients, K, are plotted versus the radius of gyration, R_G, of the small polymers in the network. Also, K for spheres of radius R_G could be calculated as the available volume fraction in the networks by numerically integrating $g(R)$ from R_G to infinity. The results of these calculations are shown as the solid lines in Figure 6. The results indicated that when we modeled the obstruction of the diffusion of small polymers, R_G could be a good estimate of the solute radius. The maximal reduction of R_G due to the network was 7%, which was found for the longest polymer in the most concentrated network. In reality this is within experimental limitations. The radii of gyration of the PEG molecules used in the experiments were calculated according to the Rouse–Zimm model,[20] assuming Θ conditions and infinite chain lengths. Accordingly, we had $R_G = 1.5R_H$, where R_H is the hydrodynamic radius of the PEGs, calculated from the diffusion coefficient in water[1] as $R_H = kT/6\pi\eta D_0$. The assumptions inherent in the calculations of R_G were verified experimentally. First, we found $D_0 \sim M_w^{-0.46}$, which is the Rouse–Zimm result. Second, using the experimentally observed $(R_0^2/M_w)^{1/2}$ = 0.93 Å,[21] where R_0^2 is the mean-squared unperturbed end-to-end distance of the chains, together with $R_G^2 = R_0^2/6$, we were able to calculate R_G for the PEG molecules. For example, R_G for the molecular weights 326 and 3978 was calculated to be 6.9 and 23.9 Å, respectively. This compared favorably with our experimental determinations of 7.3 and 23.5 Å, using $R_G = 1.5R_H$.

Finally, Figure 7 shows the analytical predictions, i.e., eq 7 with $R_s = R_G$, and our experimental results on κ-car-

rageenan[1] in three different states: in solution, as a chemically cross-linked network, and as a physically cross-linked network. In a solution, as well as in a chemically cross-linked network, the κ-carrageenan at the given concentration is in its coil conformation.[22] The coils have a persistence length above 68 Å.[23] This value is high enough for our analytical theory to be applicable, since the polymer radius $a \approx 3.3$ Å,[22] giving $p/a > 10$. The predictions, lower solid line, gave a good agreement with our experimental results which supports the use of R_G. A physically cross-linked κ-carrageenan gel, on the other hand, is suggested to be composed of aggregated double helices,[24] each helix with a radius of 5.1 Å.[22] Therefore, in the calculations (with eq 7) we used a polymer radius $a = 5.1$ Å (upper solid line). The dashed line in Figure 7 corresponds to a case where the network was assumed to contain 50% double helices and 50% coils; i.e., the radius a was set equal to 4.2 Å. This assumption gave very good agreement with the experiments. However, the detailed structure of the gel is not known and will therefore not be subjected to further discussion. In the calculations shown in Figure 7, we accounted for the hydration of the κ-carrageenan chains according to the same procedure as mentioned above.

Discussion

The fundamental parts of our theory are based on the following main assumptions: (a) the reduction of solute diffusion in polymer gels or solutions can be described in terms of steric hindrance—i.e., hydrodynamic interactions are negligible; (b) the hindrance to diffusion is due to the structure of a "static" network, not distorted by the diffusing species; (c) the structure of the network can be decomposed into a set of cylindrical cells, where the contribution from each cell to, e.g., the diffusion coefficient is determined by the "distribution of spaces in the network", i.e., $g(R)$.

Hydrodynamic interactions will always be present. However, the theory of Cukier,[3] which is based solely upon hydrodynamics, predicts a faster diffusion in a solution of rods than in a solution of random coils. This contradicts our experimental observations on PEG diffusion in solutions of poly(styrenesulfonate) at different ionic strength.[1] Our experiments were carried out at low polymer volume fraction and with rather small solutes. It was therefore likely that under these circumstances, the effects of hydrodynamics on solute diffusion were quite small. On the other hand, the agreement between our theory and the measurements of Ogston et al. on the diffusion of albumin in solutions of hyaluronic acid and dextran showed that predictions with our theory were successful, although albumin is quite a large molecule, $M_w \sim 70\,000$. For higher polymer concentrations, the hydrodynamic interactions cannot be neglected, especially not if the network through which the particles diffuse consists of immobile particles[25] or chains. Nevertheless, chemically cross-linking a polymer solution does not necessarily influence solute diffusion, as shown in Figure 7. Moreover, the calculation of the hydrodynamic interactions is quite involved and is often carried out assuming a hydrodynamic screening effect,[3,4] the physical basis of which remains to be clarified.[25]

According to postulates of statistical mechanics, the time-averaged properties of a system can be replaced by the ensemble-averaged ones. Thus, the distribution of spaces in a real network, in which the polymer chains are allowed to move, can to a good approximation be described by the procedure presented in this paper. Also, it follows that a global property, e.g., the effective diffusion coefficient or the partition coefficient (K) for a sphere partitioning between a solvent and a network, can be looked upon as the result of events in small subsystems. It should be noticed that inherent in our treatment, i.e., eq 2, lies the fact that the available volume fraction for diffusion, i.e., K, is calculated correctly independently of the choice of the local model. Thus, a calculation of K can be carried out by first decomposing the distribution of spaces into a set of subsystems and then using the appropriate expression for the contribution from each subsystem, e.g., $K(b) = (1 - (R_S + a)^2/b^2)S(R-(b-a))$ for the cylindrical cell model. This gives exactly the same result as when K is calculated directly from the distribution of spaces.

The decomposition of a network structure into a set of cylindrical cells might at first sight look rather questionable, especially if the network is composed of random coils. On the other hand, a justification for our approach was given by the agreement between the BD simulations and the predictions. Further, the shape of a plot of D/D_0 versus the polymer volume fraction, ϕ, was experimentally observed to be convex, as shown in Figure 5. This means that a small change in ϕ alters D/D_0 more at low volume fraction than at high. On the other hand, a plot of D/D_0 versus the solute radius, R_s, was concave (see Figure 7). This was also found by replotting the experimental data of Ogston et al.[9] as D/D_0 versus R_s. The results reported by Brown and Chitumbo[26] also show the same concave curvature. As can be seen in the figures, our model has indeed the qualitatively correct behavior for both cases, in contrast to the phenomenological approach by Ogston[9] and the hydrodynamic treatment by Cukier.[3] It can be mentioned that when ϕ increases toward dense packing, the plot of the theoretical D/D_0 versus ϕ changes from convex to concave, as expected.

In all our predictions we have used the radial diffusion quotient, D_r/D_0, of the cylindrical cell model, CC, and this deserves some further attention. In the "original" CC,[7] the correct expression is given as $D/D_0 = {}^1/_3 + {}^2/_3(D_r/D_0)$; i.e., the diffusion parallel to the polymer is assumed to be free. However, it can be argued that our calculations of $g(R)$ were carried out by determining the distance to the polymer chain of closest approach, i.e., the radial distance. Thus, applying this procedure on a two- or three-dimensional CC should give the same result. Also, the original CC expression gave a too high diffusion quotient when compared to Brownian dynamics simulations. Similar discrepancies have been reported by other authors for ion diffusion in polyelectrolyte solutions.[27,28] Apparently, further theoretical considerations are needed on the use of the radial diffusion quotient in isotropic systems.[29]

In our preceding paper,[1] we presented our results for D/D_0 in terms of the hydrodynamic radius, R_H, of the PEGs. In this paper we have shown that using the radius of gyration, R_G, the predictions compared better with the experiments. As the polymer volume fraction in our experiments was low, below 0.03, we expected that the PEGs would behave nearly as in free solution, and using R_G determinations in water is then appropriate. Also, the simulations of the partition coefficient for a modeled PEG polymer in networks showed that the small polymers behaved as equivalent spheres of radius R_G. These findings are in agreement with results reported by Phillies.[2] He discussed experimental results of the diffusion of polymers and of spherical probes in polymer matrices (semidilute regime). It was concluded that both nonreptating polymers and probes behave as hydrodynamic blobs of size R_G

(i.e., polymer radius of gyration and sphere radius). On the other hand, PEG molecules will experience a less hindered diffusion than equivalent spheres in more concentrated networks. This follows from the fact that polymers can move, i.e., reptate, between two obstacles spaced with an intervening distance less than R_G This is not the case for rigid spheres.

Finally, so far our discussion has concerned the basic principles of our treatment. We have shown the applicability of the theoretical approach to a number of different systems, simulated and experimental. However, we wish to stress the generality of the analytical theory, eq 7. It is applicable to networks composed of polymer chains with highly different flexibility. This follows from our findings that if the ratio of persistence length to polymer radius, p/a, is 10 or larger, the distribution of spaces, $g(R)$, in such networks is essentially the same. This has to our knowledge never been shown before. Further, $g(R)$ can to a good approximation be taken as the one given by Ogston (eq 5), accounting for a finite polymer radius. We also wish to emphasize the absence of direct scaling behavior of our analytical expression, and still it compares favorably with literature data.

Acknowledgment. L.J. was financially supported by grants to the Chalmers University of Technology from Astra Hässle AB. C.E. acknowledges financial support from the Swedish Natural Science Research Council. We are grateful to Dr. Bengt Jönsson at the University of Lund for stimulating discussions. Dr. Bob Carter, Astra Hässle AB, is acknowledged for his help with Figure 3. These were produced with the molecular modeling system SYBYL (TRIPOS Associates, Inc., St. Louis).

References and Notes

(1) Johansson, L.; Skantze, U.; Löfroth, J.-E. *Macromolecules*, preceding paper in this issue.
(2) Phillies, G. D. J. *J. Phys. Chem.* **1989**, *93*, 5029.
(3) Cukier, R. I. *Macromolecules* **1984**, *17*, 252.
(4) Altenberger, A. R.; Tirrell, M. *J. Chem. Phys.* **1984**, *80*, 2208.
(5) Jönsson, B.; Wennerström, H.; Nilsson, P. G.; Linse, P. *Colloid Polym. Sci.* **1986**, *264*, 77.
(6) Belloni, L.; Drifford, M. *Chem. Phys.* **1984**, *83*, 147.
(7) Nilsson, L. G.; Nordenskiöld, L.; Stilbs, P.; Braunlin, W. H. *J. Phys. Chem.* **1985**, *89*, 3385.
(8) Phillips, C. G.; Janssons, K. M. *Macromolecules* **1990**, *23*, 1717.
(9) Ogston, A. G.; Preston, B. N.; Wells, J. D. *Proc. R. Soc. London, A* **1973**, *333*, 297.
(10) Ogston, A. G. *Trans. Faraday Soc.* **1958**, *54*, 1754.
(11) Giddings, J. C.; Kucera, E.; Russell, C. P.; Myers, M. N. *J. Phys. Chem.* **1968**, *72*, 4397.
(12) Limbach, K. W.; Nitsche, J. M.; Wei, J. *AIChE. J.* **1989**, *35*, 42.
(13) Schellman, J. A. *Biopolymers* **1974**, *13*, 21.
(14) Hagerman, P. J.; Zimm, B. H. *Biopolymers* **1980**, *20*, 1481.
(15) McQuarrie, D. *Statistical Mechanics*; Harper & Row: New York, 1976.
(16) Cleland, R. L. *Arch. Biochem. Biophys.* **1977**, *180*, 57.
(17) Guizard, C.; Chanzy, H.; Sarko, A. *Macromolecules* **1984**, *17*, 100.
(18) Thalberg, K. Doctoral Thesis, University of Lund, Lund, 1990.
(19) Garg, S. K.; Stivala, S. S. *J. Polym. Sci., Polym. Phys. Ed.* **1978**, *16*, 1419.
(20) Fujita, H. *Polymer Solutions*; Elsevier: New York, 1990.
(21) Allen, B.; Booth, C.; Hurst, S. J.; Jones, M. N.; Price, C. *Polymer* **1967**, *8*, 391.
(22) Nilsson, S.; Piculell, L.; Jönsson, B. *Macromolecules* **1989**, *22*, 2367.
(23) Slootmaekers, D.; De Jonghe, C.; Reynaers, H.; Varkevisser, F. A.; Bloys van Treslong, C. J. *Int. J. Biol. Macromol.* **1988**, *10*, 160.
(24) Millane, R. P.; Chandrasekaran, R.; Arnott, S. *Carbohydr. Res.* **1988**, *182*, 1.
(25) Carter, J. M.; Phillies, G. D. J. *J. Phys. Chem.* **1985**, *89*, 5118.
(26) Brown, W.; Chitumbo, K. *J. Chem. Soc., Faraday Trans. 1* **1975**, *71*, 1.
(27) Bratko, D.; Stilbs, P.; Bester, M. *Makromol. Chem., Rapid Commun.* **1985**, *6*, 163.
(28) Piculell, L.; Rymdén, R. *Macromolecules* **1989**, *22*, 2376.
(29) Phillips, C. G. Doctoral Thesis, University of Cambridge, Cambridge, 1987.